Fast Ion Production by Laser Filamentation in Laser-Produced Plasmas

P. E. Young, G. Guethlein, S. C. Wilks, J. H. Hammer, W. L. Kruer, and K. G. Estabrook
Lawrence Livermore National Laboratory, University of California, P.O. Box 5508, Livermore, California 94550
(Received 20 November 1995)

Production of protons with energies of ~20 keV have been observed to originate from the interaction of a high intensity laser with a preformed underdense plasma. The energy and distribution of ions are explained by acceleration by the ponderomotive force resulting from filamentation. [S0031-9007(96)00010-5]

PACS numbers: 52.40.Nk, 52.35.Fp, 52.35.Mw, 52.50.Jm

The propagation of high intensity laser pulses through plasmas has been studied for a number of years. Predictions of laser-target interactions for inertial confinement fusion (ICF) applications, for example, will change if the laser intensity is sufficiently high to form density channels via the ponderomotive force or exceed the threshold for the filamentation instability. Numerous theoretical works have studied filamentation at low intensities [1]. Presently nonlinear fluid simulations [2,3] are being used to simulate high intensities ($>10^{16}$ W/cm^2) which can occur in ICF applications; it is important to experimentally verify their accuracy in this new regime. Experimental measurement of filamented density channels formed at high intensities is extraordinarily difficult via imaging techniques due to their small transverse dimensions (~10 μm). On the other hand, as shown first in particle-in-cell simulations [4] and in the fluid simulations [2,3], intense laser pulses can produce a large transverse ponderomotive force which can accelerate ions to high velocities ($v_i \gg c_s$, the sound speed) which can then be used to diagnose the laser intensity in the filament. Although the energy distributions of ions ejected from laser-plasma interactions have been studied extensively in the past [5], these ions have generally been accelerated by the ambipolar potential created by hot electrons which can be produced by processes such as resonance absorption [6].

In this Letter, we describe the results of an experiment in which ion velocity distributions are observed which are produced when a focused laser beam interacts with preformed underdense plasmas. As we vary the incident laser intensity, the production of hot ions is correlated with the onset of filamentation. The separation of the plasma formation from the hot ion generation allows us to distinguish between the ion distributions from each process and to choose the maximum electron density reached by the interaction beam. We have observed proton energies of ~20 keV for incident intensities of 5×10^{16} W/cm^2, a laser wavelength of 1.064 μm, and densities of $0.25 n_c$, where n_c is the critical density at which the incident laser frequency equals the electron plasma frequency. This result is confirmed by two-dimensional fluid simulations, which show that the ion ejection is localized spatially to the filamentation region, and by particle-in-cell simulations which accurately predict the observed ion energies.

A simple estimate shows that filamentation can easily produce ions with energies much greater than the initial thermal ion energy. We equate the kinetic energy of the ion to the potential energy set up by the ponderomotive force $M v_{\max}^2/2 \simeq Ze\phi \simeq Zm v_{\rm os}^2/4$, where M is the ion mass, m is the electron mass, ϕ is the ponderomotive potential, and $v_{\rm os} = eE/m\omega_0$ is the electron oscillatory velocity in a laser electric field E with a frequency ω_0. Solving for $v_{\max}$ gives

$$v_{\max} \simeq \sqrt{Zm/2M}\; v_{\rm os}\,. \tag{1}$$

For hydrogen ($Z = 1, m/M = 1/1836$), and $I_L = 1.5 \times 10^{17}$ W/cm^2, which results from filamentation of the laser light in the plasma (discussed below), we find $v_{\max} = 1.7 \times 10^8$ cm/s, which corresponds to an energy of 15 keV; for comparison, a typical c_s and ion temperature for the plasmas we will be discussing will be 3×10^7 cm/s and 500 eV, respectively. For a filament diameter of 10 μm, and a pulse length of 100 ps, as discussed below, an ion with a velocity of 1×10^7 cm/s can move from the center to the edge of the filament, so even thermal ions will have time to move out of the channel.

Most previous experiments [5] measured the ion energies with Faraday cups which cannot distinguish between different ion species. Hydrogen ions with energies up to 180 keV have been reported [7] with a laser intensity of 10^{16} W/cm^2, however, this was performed with a single laser beam on an overdense target, so it is difficult to separate out the hot ions produced in the underdense plasma from those produced by interaction of the laser pulse with the critical density surface.

The present experiment was conducted using the Janus laser at Lawrence Livermore National Laboratory where we have developed a test bed for studying the propagation of moderately intense laser pulses through well-characterized underdense plasmas [8]. A 1.064 μm wavelength, 100 ps full width at half maximum (FWHM) Gaussian pulse of intensity $\leq 5 \times 10^{16}$ W/cm^2 interacted with an underdense plasma formed by the irradiation of a 0.5 μm thick parylene [$(CH)_n$] foil by a 1 ns, 0.532 μm wavelength, 400 μm diameter, 2×10^{13} W/cm^2 laser

 0031-9007/96/76(17)/3128(4)$10.00

pulse. The interaction beam at best focus has a single central spike of full width half energy of 13 μm, is circularly symmetric, and has a confocal parameter of 200 μm [9]. Varying the relative timing between the two pulses (1.5 to 2.5 ns delay from the end of the plasma forming pulse) determined the peak density ($0.25n_c$ to $0.1n_c$) seen by the interaction pulse. The background density profile was measured using a folded-wave interferometer that used a 50 ps, 0.35 μm wavelength probe pulse that arrived at the target at the same time as the peak of the 100 ps interaction pulse.

The ion velocities were measured at 90° to the incident laser beams by a time resolved ion spectrometer [10] which used a magnetic field to separate ions of different charge-to-mass ratios. The ions pass through a collimating slit and strike a microchannel plate so that an optical streak camera can be used to measure the ion time of flight. An example streak is shown in Fig. 1 for a case with the interaction beam; the protons produced with the interaction beam (33 J) have velocities twice that without the beam for a factor of 4 increase in energy (8 to 32 keV). The arrival of the laser pulses at the target is marked by the x-ray emission feature in the upper left hand corner of the streak. Although the electron temperatures are high enough (0.5–1 keV from LASNEX [11] simulations and Thomson scattering measurements [12]) that the carbon ions are fully ionized, multiple charge states of carbon are observed because there are enough residual neutrals (base pressure $\leq 10^{-5}$ Torr) between the plasma and the ion spectrometer for the ions to pick up electrons via charge exchange. The ion time of flight was also measured at various angles using Faraday cups. The peak ion energy normal to the target is independent of the interaction beam energy, whereas transverse to the beam accelerated ions is seen, as expected if filamentation is the acceleration mechanism.

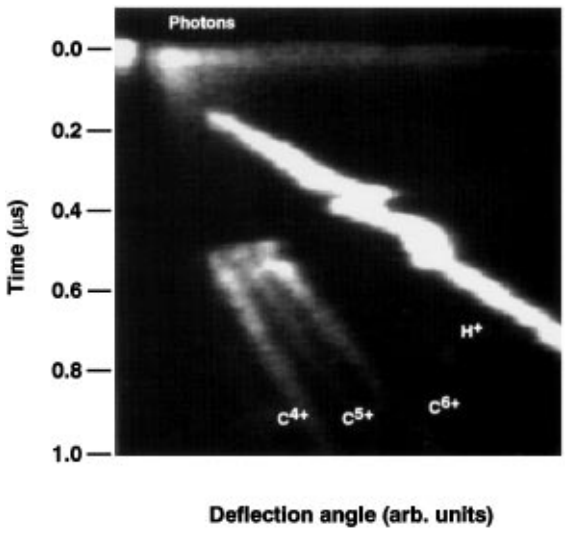

FIG. 1. A sample ion spectrometer streak with the interaction beam incident on a CH foil target.

When the interaction beam is of sufficient energy, a high energy proton tail forms with peak energies of ~20 keV. These ions are sufficiently energetic to have ion-ion mean free paths which are greater than the plasma diameter (400 μm). Using Eqs. (5-31) of Ref. [13], we find that 20 keV protons moving through a background of 500 eV carbon ions (from LASNEX [11] simulations) at an ion density of 3.6×10^{19} cm^{-3} have a mean free path of about 5.0 mm. The proton energy has to drop below 6 keV for the mean free path to equal 400 μm.

We also monitored the levels of the three dominant underdense plasma processes: filamentation, stimulated Brillouin scattering (SBS) in which an ion acoustic wave couples to the incident light wave and a reflected light wave, and stimulated Raman scattering (SRS) in which an electron plasma wave couples to the incident light wave and a reflected light wave. We will next describe the measurement techniques for each of these before discussing the experimental results.

The onset of the filamentation instability is determined from measurements of the light transmitted through the plasma. The light from the interaction beam that is transmitted through the plasma is collected with an $f/2$ lens and relayed to a full aperture energy calorimeter; since the interaction beam is focused with an $f/2$ lens, in the absence of deflections, all the incident laser light is collected by the calorimeter with the exception of backscattered light. As we have observed in earlier work [3,9], when the beam breaks up into filaments, the density grating set up by the filaments deflects light out of the collection solid angle, leading to a decrease in the ratio of measured transmitted energy to the incident energy.

The SBS energy is measured for the entire experiment using a beam splitter which directs 4% of the light backscattered into the focusing lens to a calorimeter. A dielectric mirror for 0.53 μm light rejects energy from the plasma forming beam which might leak through the plasma. Spectral analysis of the backscattered light has shown it to be shifted and significantly broadened in wavelength compared to the incident light, which is expected for SBS light.

The SRS light backscattered into the focusing lens was measured for a limited portion of the experiment. A fast pyroelectric detector was spectrally filtered to respond to scattered light wavelengths that corresponded to SRS at densities between $0.1n_c$ and $0.2n_c$. The backscattered 1.064 μm light was reduced by dielectric mirrors which provided an attenuation of $>10^6$ for a 100 nm band of wavelengths centered on the laser wavelength.

We now discuss the results of our measurements of the three instabilities, and we find that filamentation best describes our observations. Since the filamentation threshold predicted by theory [14] is inversely proportional to density, as one lowers the peak density, the laser intensity has to be increased to reach the filamentation threshold. Our measurements in this experiment show that filamentation

appears at 5 J for $n_e = 0.25n_c$, 15 J for $n_e = 0.15n_c$, and 25 J for $n_e = 0.1n_c$ as shown in Fig. 2(a). Note that the high transmission at low energies confirms that the entire pulse interacts with a completely underdense plasma and that the plasma absorption is low. For the plasma conditions of this experiment, the inverse bremsstrahlung absorption length is >1 mm [9].

From Fig. 2, we see that the increase in ion energy is coincident with the onset of the filamentation instability. As the laser energy is increased, the peak ion energy first increases with the laser energy, then reaches a constant value when the peak density is $0.25n_c$. If the peak density is reduced to $0.15n_c$, the input energy has to be increased before the ion energy increases, but at 30 J we attain the same ion energy as at the higher density.

When SRS is strongly driven, the electron plasma waves (EPW's) can accelerate a significant number of hot electrons, which in turn create a potential which accelerates ions. The EPW's for backscattered and sidescattered SRS can accelerate electrons to energies in the range of 1 to 100 keV [15]. We observe no correlation, however, between the level of SRS backscattered light, which is a direct product of the instability, and the peak ion energy.

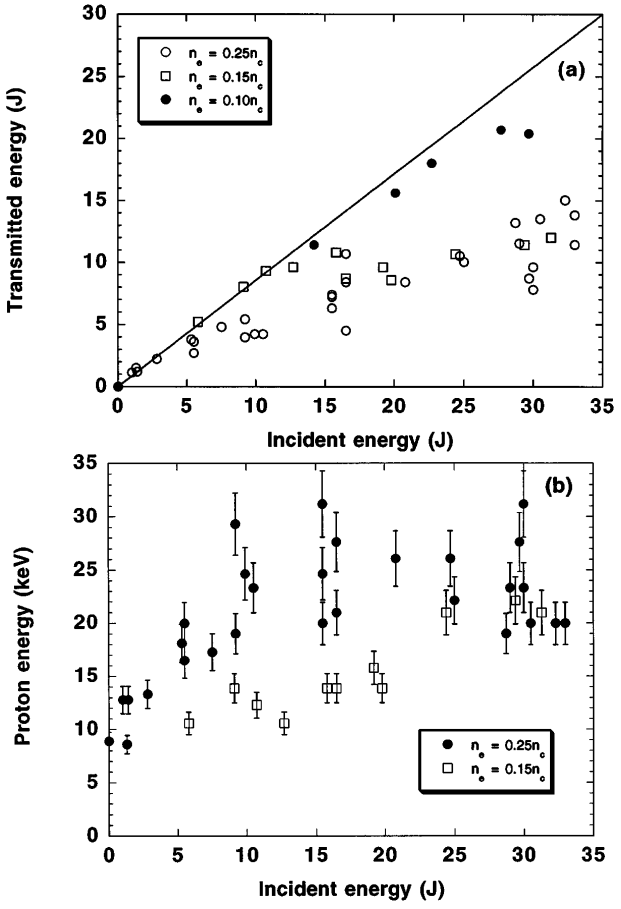

FIG. 2. Comparison of the onset of (a) scattering of the transmitted light due to filamentation, and (b) an increase in the peak proton energy as a function of incident energy.

For example, for an input laser energy of 30 J, there is a factor of 100 decrease in SRS scattered level when the peak density is decreased from $0.25n_c$ to $0.1n_c$ with no significant drop in the peak ion energy.

SBS is also known to accelerate ions, however, it is difficult to explain the observed ion energies based on known nonlinear SBS behavior. Saturation of SBS by ion trapping, e.g., can accelerate ions to velocities comparable to the ion wave phase velocity ($\sim 2c_s$) [16]. The sound speed is determined by the carbon ions [17], so the kinetic energy of the protons is $M_H(2c_s)^2/2 = 4Z_H T_e$, or only about 4 keV. The backscattered energy levels do show a behavior similar to that of the proton energy, but this is probably in response to the higher laser intensities in the filaments which have been observed in simulations [18].

We have investigated this phenomenon with two-dimensional LASNEX [11] simulations. The simulation is approximated as a Cartesian x-y system by setting up the problem at a large radius ($r = 1$ cm) of the normal r-z LASNEX coordinate system; this means that the problem is not exactly symmetric about the laser axis, which leads to slight asymmetries in the way the beam propagates. In the simulation, the 100 ps interaction laser propagates into an underdense plasma with a parabolic density profile with a peak density of $0.25n_c$. The initial electron temperature is 1 keV and the initial ion temperature is 500 eV.

The simulation shows that there is a region of localized ion heating (see Fig. 3) in the area where the interaction beam begins to break up into filaments. The location of the beam breakup agrees well with the measured location of the end of the density channel in this and previous experiments [3,9]. For the simulation shown, the incident intensity is 5×10^{16} W/cm^2, and at the peak of the pulse the ion temperatures have risen above 2 keV. The laser light has filamented to peak intensities near 1.3×10^{17} W/cm^2 producing radial plasma motion of 1×10^8 cm/s (hydrogen energy ~ 20 keV). The ion heating is then understood in terms of shock heating of the background ions.

LASNEX shows a gradual increase of ion temperature with incident energy between the onset of filamentation and saturation, which agrees qualitatively with experiment, although saturation is reached for higher incident energies of ~ 25–30 J. The difference may be due to the focusing f/number (f/∞ in the simulation) or the difference in the filamented intensity between the 2D simulation and the 3D experiment. Physically, the saturation occurs because of the evacuation of the channel; when the laser intensity reaches 1.3×10^{17} W/cm^2, for example, then $v_0^2/v_e^2 \sim 40$, so $n/n_0 \sim \exp[-(v_0/v_e)^2/4] \sim e^{-10}$, and there are few ions to accelerate.

The fluid description in LASNEX provides valuable insight into the filamentation of the laser light and the formation of the density channels; however, it gives an average, rather than two-species, ion description of the plasma response. Since the mean free path is long, one actually expects interpenetration of the ion species. Hence, to see the

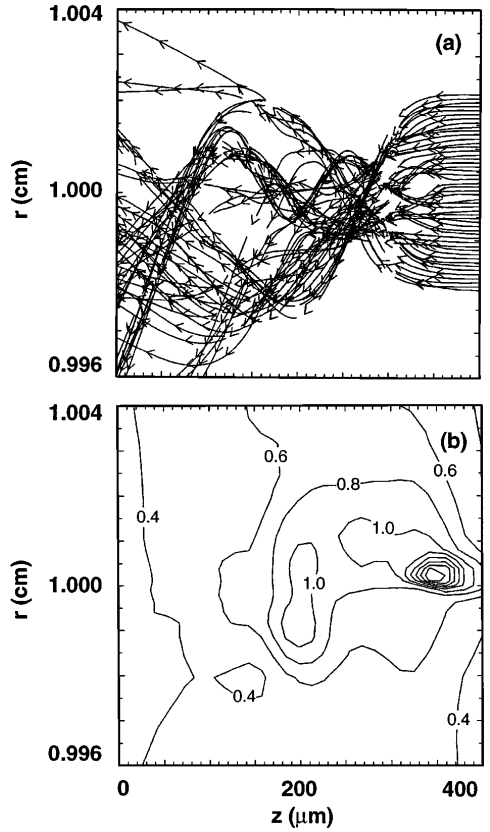

FIG. 3. LASNEX simulations comparing (a) the interaction laser rays to (b) the ion temperature spatial distribution at the peak of the interaction pulse.

details of the ion distribution, we complement LASNEX with an electron-fluid particle ion code (EPIC) [19]. In the EPIC simulation, the plasma consisted of equal amounts of carbon ($Z = 6, A = 12$) and hydrogen ($Z = 1, A = 1$) ions. This system was chosen such that the ion dynamics in a transverse slice could be studied in detail. This slice is at the x position of 335 μm in Fig. 3(a), corresponding to the beginning of the filamentation region. The intensity distribution along this slice was obtained from the LASNEX simulation described above and was input into EPIC; the peak intensity was 1.3×10^{17} W/cm^2 with an intensity modulation of 50% with a modulation period of 10 μm. The average plasma density at this point is 10^{20} cm^{-3}. This intensity profile was ramped up from zero to its maximum value over a time of $\sim$50 ps. The electron temperature, chosen to be 1 keV, was fixed. Figure 4 shows the resulting ion phase space for the hydrogen ions. The ion energies for both carbon (not shown) and hydrogen are in agreement with those measured in the experiment for the same conditions. For example, the experiments measure a velocity for the hydrogen ions that is about a factor of 2 faster than the carbon ions; this is also found in the simulations, and is in agreement with the scaling of Eq. (1).

In summary, we have shown that filamentation enhances ion energies significantly. This produces further validation of the codes in high intensity and filamentary regimes, and demonstrates a potential diagnostic of the laser intensity in the plasma.

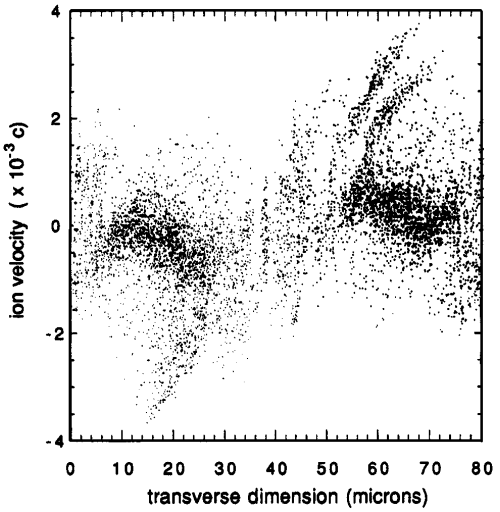

FIG. 4. Phase space plot of EPIC results for hydrogen.

We thank J. Bonlie, W. Cowens, R. Gonzales, and G. London for technical assistance. This work was performed under the auspices of the U.S. Department of Energy by the Lawrence Livermore National Laboratory under Contract No. W-7405-Eng-48.

[1] R. Rankin *et al.,* Phys. Rev. Lett. **63**, 1597 (1989); E. M. Epperlein, *ibid.* **65**, 2145 (1990); A. J. Schmitt, Phys. Fluids **3**, 186 (1991); T. M. Antonsen and P. Mora, Phys. Rev. Lett. **69**, 2204 (1992); M. Amin *et al.,* Phys. Fluids B **5**, 3748 (1993); H. A. Rose and D. F. Dubois, Phys. Rev. Lett. **72**, 2883 (1994).
[2] R. L. Berger *et al.,* Phys. Fluids B **5**, 2243 (1993); **5**, 1935 (1993).
[3] S. C. Wilks *et al.,* Phys. Rev. Lett. **73**, 2994 (1994).
[4] W. B. Mori *et al.,* Phys. Rev. Lett. **60**, 1298 (1988).
[5] S. J. Gitomer *et al.,* Phys. Fluids **29**, 2679 (1986), and references therein.
[6] A. V. Gurevich *et al.,* Zh. Eksp. Teor. Fiz. **63**, 516 (1972) [Sov. Phys. JETP **36**, 274 (1973)].
[7] R. Decoste and B. H. Ripin, Phys. Rev. Lett. **40**, 34 (1978).
[8] P. E. Young *et al.,* Phys. Rev. Lett. **75**, 1082 (1995).
[9] P. E. Young *et al.,* Phys. Plasmas **2**, 2825 (1995).
[10] G. Guethlein *et al.* Rev. Sci. Instrum. **66**, 333 (1995).
[11] G. D. Zimmerman and W. L. Kruer, Comments Plasma Phys. Controlled Fusion **2**, 51 (1977).
[12] P. E. Young, Phys. Rev. Lett. **73**, 1939 (1994).
[13] L. Spitzer, Jr., *Physics of Fully Ionized Gases* (Interscience, New York, 1962), 2nd ed., p. 135.
[14] W. L. Kruer, Comments Plasma Phys. Controlled Fusion **9**, 63 (1985).
[15] D. W. Phillion *et al.* Phys. Fluids **25**, 1434 (1982).
[16] W. L. Kruer *et al.,* Phys. Rev. Lett. **35**, 1076 (1975).
[17] E. A. Williams *et al.,* Phys. Plasmas **2**, 129 (1995).
[18] V. V. Eliseev *et al.,* Phys. Plasmas **2**, 1712 (1995).
[19] S. C. Wilks *et al.,* Phys. Rev. Lett. **74**, 5048 (1995).